

Superpositions of SU(3) coherent states via a nonlinear evolution

K. Nemoto¹[†] and B. C. Sanders²¹

¹*Centre for Quantum Computer Technology, The University of Queensland, Queensland 4072, Australia*

²*Department of Physics, Macquarie University, Sydney, New South Wales 2109, Australia*

(Dated: October 30, 2018)

We show that a nonlinear Hamiltonian evolution can transform an SU(3) coherent state into a superposition of distinct SU(3) coherent states, with a superposition of two SU(2) coherent states presented as a special case. A phase space representation is depicted by projecting the multi-dimensional Q -symbol for the state to a spherical subdomain of the coset space. We discuss realizations of this nonlinear evolution in the contexts of nonlinear optics and Bose–Einstein condensates.

INTRODUCTION

The superposition principle in quantum physics implies that superpositions of probability amplitudes for classical-like states are possible, yet superpositions of quasi-classical quantum field states are not generally observed in practice. Such superposition states are especially interesting as they dramatically illustrate the quantum superposition principle by creating coherent superpositions of distinct states, with these distinct states behaving as classical physical states. Extensive theoretical and experimental studies have been directed towards understanding and obtaining superpositions of distinct quasi-classical states, often referred to as Schrödinger cat states[1, 2]. In general the interest has been in generating superpositions of Heisenberg–Weyl coherent states via a nonlinear Hamiltonian evolution [1, 3], where the Heisenberg–Weyl coherent states are the displaced harmonic–oscillator vacuum state.

Heisenberg–Weyl coherent states are relevant for studying the quantum–classical transition for the harmonic oscillator with one degree of freedom. The generalization to harmonic oscillators with two or more degrees of freedom leads to superpositions of product coherent states, or entangled coherent states, with a wealth of phenomena to be studied for such systems[4]. However, another generalization of superpositions of coherent states is possible by employing the generalized coherent states for general group actions[5]. Examples include superpositions of SU(2) coherent states[6] and superpositions of SU(1,1) coherent states[7], as well as superpositions of multiparticle SU(2) and SU(1,1) coherent states[8]. Whereas the Heisenberg–Weyl group is the symmetry group for harmonic oscillators, SU(2) is the symmetry group for spin precession, for two–channel interferometry and for the dynamics of ideal two–level atoms[5, 9, 10, 11], and SU(1,1) is the symmetry group for the production of squeezed light and quantum interferometry with parametric up– and down–conversion[7, 11]. The generalized coherent states for such systems represent the quasi-classical states. For example the SU(2) coherent states are also known as atomic coherent states and are analogous to classical electric dipoles[10]. Superpositions of these generalized coherent states in quantum systems are therefore of interest in studying counter-intuitive manifestations of the superposition principle.

The studies of superpositions of Heisenberg–Weyl, SU(2) and SU(1,1) coherent states are simplified by the fact that these are one–parameter groups, and the corresponding coset space is thus a locally two–dimensional manifold. For the Heisenberg–Weyl group, the manifold is the plane, for SU(2) the Poincaré sphere and for SU(1,1) the Lobachevsky plane. Here we generalize the studies of superpositions of coherent states to a two–parameter Lie group, namely SU(3). The manifold for phase space dynamics is the four–dimensional space isomorphic to the coset space SU(3)/U(2). Working in a manifold which is greater than two dimensions presents problems in terms of visualizing the dynamics, which we resolve by projecting the dynamics to subdomains of spherical manifolds.

In order to generate superpositions of SU(3) coherent states, we consider the three–dimensional nonlinear oscillator. Such a model can be realized by employing the three–boson realization of the SU(3) generators and constructing the dynamics optically through employing passive optical devices and Kerr–type nonlinearities. Another physical system involves three interacting, independent Bose–Einstein condensates (BECs) [12]. In order to bring out the essential properties of superpositions of SU(3) coherent states, we treat the dynamics as a closed system.

Superpositions of SU(3) coherent states may be interesting from the perspective of weak force detection and accurate measurements. For example, weak force detection for two coupled, separated BECs employs a superposition of two extremal SU(2) coherent states[13]. Superpositions of two extremal SU(2) coherent states are valuable for related applications, such as precision measurement in particle interferometry[14]. Symmetries of SU(3) coherent states may also prove to be valuable in the context of weak force detection for three coupled BECs or for three–channel particle interferometry, as examples.

We show that an initial SU(3) coherent state in the nonlinear oscillator evolves to a superposition of SU(3) coherent states. An analytical solution is provided which shows explicitly that a superposition of sixteen SU(3) coherent states

occurs. The analytical solutions for the SU(3) case are more complex and interesting than those for SU(2), and we elaborate on the superposition of two SU(2) coherent states as a special case. Graphical solutions are employed by using the Q -symbol (sometimes referred to as the Q -function) for the state and projecting to spherical subdomains. The graphical method provides an intuitive picture of the dynamics.

THREE-DIMENSIONAL NONLINEAR OSCILLATOR

The Hamiltonian for the three-dimensional nonlinear oscillator includes three pairs of annihilation and creation operators, designated by $\hat{c}_1, \hat{c}_1^\dagger, \hat{c}_2, \hat{c}_2^\dagger, \hat{c}_3, \hat{c}_3^\dagger$, with each pair $\{c_i, c_i^\dagger\}$ corresponding to one degree of freedom, or “mode”. The usual boson commutation relation $[\hat{c}_k, \hat{c}_j^\dagger] = \delta_{kj}$ applies. We also define number operators as $\hat{n}_k = c_k^\dagger c_k$, and a total number operator $\hat{N} = \sum_{k=1}^3 \hat{n}_k$. We consider an isolated system; hence, total energy and total particle number are conserved. In particular we are interested in the simplest system with energy and number conservation which will allow an SU(3) coherent state to evolve into a superposition of SU(3) coherent states. Such a Hamiltonian is given by

$$H = \omega \sum_{k=1}^3 \hat{n}_k + \chi_1(t) \sum_{k=1}^3 \hat{n}_k^\dagger (\hat{n}_k - 1) + \chi_2(t) \sum_{\substack{j,k=1 \\ j \neq k}}^3 \hat{n}_k \hat{n}_j + \sum_{\substack{j,k=1 \\ j \neq k}}^3 \Omega_{jk}(t) c_j^\dagger c_k, \quad (1)$$

with $\Omega_{jk}(t) = \Omega_{kj}^*(t)$. In this model, the coupling constant χ_1 corresponds to the strength of the self-modulation term, and χ_2 is the strength of the cross-modulation term. The time-dependent quantities χ_i are assumed to be controllable as well as the time-dependent coupling strengths Ω_{jk} that are responsible for linear coupling between modes. For the case that each mode corresponds to bosons in a particular spatial region, the terms χ_i quantify the nonlinear interactions, and Ω_{jk} quantify the strength of (linear) quantum tunneling of bosons between modes. For $\chi_i = 0$, with $i = 1, 2$, the Hamiltonian (1) is a linear combination of su(3) generators, and thus the evolution is linear.

The Hamiltonian (1) corresponds to two potential physical realizations, the first being a nonlinear optical four-wave mixing medium, that is a medium with a $\chi^{(3)}$ nonlinearity. In four-wave mixing, the three boson operators c_k correspond to single-mode fields interacting in the medium, and the coefficients χ_i , $i \in \{1, 2\}$ are obtained by judiciously constructing the $\chi^{(3)}$ tensor coefficients.

A second realization arises in the context of interacting BECs with a small number of particles[12, 15], which is of interest for some condensates [16]. The three boson operators correspond to localized BEC modes with some overlap between the modes (in contrast to the case considered in Ref. [12], which assumes a negligible overlap). The localized modes are centered around the three minima of a three-dimensional trapping potential for the BEC. The nonlinear interactions arise due to atomic collisions and conserve boson number. The coefficients for the nonlinear interactions are χ_1 , for self interactions, and χ_2 , for intermodal collisions. These parameters depend on the s -wave scattering length for the condensate and its density as well as the degree of overlap between modes for χ_2 . These coefficients of nonlinear dynamical terms are time-dependent: the scattering length can be varied by applying an external magnetic field to exploit a Feshbach resonance in the collisions between the atoms[17].

The time-varying linear quantum tunneling terms for the BEC, with coefficients Ω_{jk} , may be varied by modifying the optical potential barrier between minima of the trapping potential. The terms are left on for a short time to produce the desired SU(3) coherent state and then shut off. Of course they are not completely eliminated as some overlap is needed for the cross-mode collisions (with coefficient χ_2) to take place. It is important that the collision terms be strong enough to be nonnegligible even when linear quantum tunneling may be ignored. Tuning the scattering length is advantageous to ensure that the intermodal collision term is sufficiently strong. Although χ_2 might be weak, our subsequent analysis is valid for any choice of χ_2 .

A typical initial condition could be N bosons in one region or mode. Allowing the system to evolve under the Hamiltonian (1) with $\chi_i = 0$, causes the system to evolve linearly, via coherent quantum tunneling, to a Perelomov SU(3) coherent state[5]. As a special case, relevant to weak force detection[13] and particle interferometry[14], extremal coherent states are states which are mapped to zero under a ladder operator. For example, the SU(2) coherent state $|j, j\rangle$ is annihilated by the specified raising operator J_+ , and the state $|j, -j\rangle$ is annihilated by the specified lowering operator J_- . These two states are extremal, and a superposition of these two extremal states would be $(|j, j\rangle + |j, -j\rangle)/\sqrt{2}$. Extremal SU(3) coherent states are states which can be annihilated by the su(3) ladder operators.

From conservation of the total number N of bosons, the Hamiltonian may be rewritten in terms of the SU(3) generators and the total number N is the irreducible representation (irrep) parameter. The eight generators of SU(3)

may be defined as the two Cartan operators

$$X_1 = \hat{c}_1^\dagger \hat{c}_1 - \hat{c}_2^\dagger \hat{c}_2, \quad (2)$$

$$X_2 = \frac{1}{3}(\hat{c}_1^\dagger \hat{c}_1 + \hat{c}_2^\dagger \hat{c}_2 - 2\hat{c}_3^\dagger \hat{c}_3) \quad (3)$$

and the six generators

$$Y_k = i(\hat{c}_k^\dagger \hat{c}_j - \hat{c}_j^\dagger \hat{c}_k) \quad (4)$$

$$Z_k = \hat{c}_k^\dagger \hat{c}_j + \hat{c}_j^\dagger \hat{c}_k, \quad (5)$$

where $k = 1, 2, 3$ and $j = k \bmod 3 + 1$. The raising operators and lowering operators are defined as

$$J_+^k = \hat{c}_k^\dagger \hat{c}_j, \quad (k < j), \quad (6)$$

$$J_-^k = \hat{c}_k^\dagger \hat{c}_j, \quad (k > j), \quad (7)$$

or, alternatively, for $k < j$

$$J_+^k = \frac{1}{2}(Z_k - iY_k) \quad (8)$$

$$J_-^k = \frac{1}{2}(Z_k + iY_k), \quad (9)$$

in terms of SU(3) generators.

The term involving the irrep parameter N can be removed by moving to a rotating picture. Furthermore, by assuming that the initial SU(3) coherent state has been generated from the evolution (1), with large linear quantum tunneling and negligible contributions from nonlinear evolution, the optical potential barrier between trapping potential minima is increased to reduce the linear tunneling. At the same time, the nonlinear coefficients must be reasonably large compared to the coefficient for linear tunneling, perhaps by employing an external magnetic field to exploit a Feshbach resonance, as discussed above. For large nonlinearities and small linear quantum tunneling terms, the Hamiltonian (1) can be approximated by

$$H = \frac{\chi}{2}(X_1^2 + 3X_2^2), \quad (10)$$

with $\chi = \chi_1 - \chi_2$. The Hamiltonian is a sum of quadratic forms of Cartan operators which commute, and this property will be useful in later calculations.

COHERENT STATES

SU(2) coherent states

In order to introduce the SU(3) coherent states, it is useful to review the SU(2) coherent states and to use this knowledge to generalize to SU(3) coherent states. SU(2) coherent states and their methods were first developed as atomic coherent states [9, 10] to treat atomic systems. On the other hand, coherent states for Lie groups were defined by Perelomov[5] as an orbit generated by group action on a reference state, which is usually the highest- (or lowest-) weight state. For compact groups, the simplest nontrivial case is SU(2), which can be parametrized by three real parameters $\{\theta, \varphi_1, \varphi_2\}$. The lowest-order faithful representation of an arbitrary $g \in \text{SU}(2)$ is as a 2×2 matrix

$$g(\varphi_1, \theta, \varphi_2) = \begin{pmatrix} e^{i\varphi_1} \cos \theta & e^{i\varphi_2} \sin \theta \\ -e^{-i\varphi_2} \sin \theta & e^{-i\varphi_1} \cos \theta \end{pmatrix}. \quad (11)$$

As $\text{SU}(2) \subset \text{SU}(3)$, the three generators of SU(2) can be obtained from (2), (3), (4) and (5). For example, the subgroup $\text{SU}(2)_{12}$ is generated by $\{X_1, Y_1, Z_1\}$. The Casimir invariant is $J^2 = X_1^2 + Y_1^2 + Z_1^2$ with eigenvalue $j(j+1)$. The 2×2 representation corresponds to $j = 1/2$. The weight basis corresponds to $|jm\rangle$ with $J_z|jm\rangle = m|jm\rangle$. The highest-weight state is $|jj\rangle$ for which $J_+|jj\rangle = 0$.

The SU(2) coherent state, for fixed j , is given by

$$|\theta, \varphi\rangle = \exp\left[-\frac{\theta}{2}(J_+^1 e^{-i\varphi} - J_-^1 e^{i\varphi})\right] |jj\rangle. \quad (12)$$

The coherent state can be represented geometrically on the Poincaré sphere, which is isomorphic to the coset space $\text{SU}(2)/\text{U}(1)$.

SU(3) coherent states

The SU(3) coherent states may be formulated as a generalization of the SU(2) coherent states[18, 19], and are obtained by the action of SU(3) on the highest-weight state. In order to obtain the SU(3) coherent states, it is convenient to employ the decomposition of SU(3) in Ref. [20], whereby the SU(3) operator is decomposed into a combination of SU(2) operators. The decomposition allows us to parameterize an arbitrary element g in the 3×3 matrix representation as

$$g = \begin{pmatrix} 1 & 0 & 0 \\ 0 & & \\ 0 & V & \end{pmatrix} \begin{pmatrix} e^{i\varphi} \cos \theta & -\sin \theta & 0 \\ \sin \theta & e^{-i\varphi} \cos \theta & 0 \\ 0 & 0 & 1 \end{pmatrix} \begin{pmatrix} 1 & 0 & 0 \\ 0 & & \\ 0 & W & \end{pmatrix}, \quad (13)$$

where $V(\varphi_1, \xi, \varphi_2)$ and $W(\varphi_3, \zeta, \varphi_4)$ are 2×2 matrices representing elements of $SU(2)_{23}$. The middle matrix on the right-hand side of Eq. (13) is an element of $SU(2)_{12}$.

The SU(3) generators of Eqs. (2,3) and (4,5) are presented as a three-boson realization. It is convenient to employ the basis states, which are eigenstates of the SU(3) Casimir operators and of the two elements of the Cartan subalgebra (2,3). The basis state can be labeled by the three numbers n_1, n_2 and n_3 , which satisfy

$$\hat{n}_k |n_1, n_2, n_3\rangle = n_k |n_1, n_2, n_3\rangle, \text{ for } k \in \{1, 2, 3\}. \quad (14)$$

As any action of the raising operators on the state $|N, 0, 0\rangle$ annihilates it, the state $|N, 0, 0\rangle$ is a highest-weight state. Coherent states are obtained by SU(3) action on this highest-weight state.

Taking the highest-weight state $|N, 0, 0\rangle$ as the reference state, the action of Eq. (13) on the highest-weight state gives an explicit form of coherent states. The factorization (13) ensures that the matrix on the furthest right leaves the highest-weight state invariant, and only the two other matrices are important in determining the coherent state. The highest-weight state is thus invariant under $SU(2)_{23}$; hence the coherent states are parametrized on the coset space $SU(3)/SU(2)$. In fact the SU(3) coherent states can be parametrized on the coset space $SU(3)/U(2)$ by eliminating an arbitrary phase, but the following calculations are easier if we retain the phase. In calculations of the Q -symbol for the state, this phase is not important.

The coherent states can be generated as

$$|\xi, \theta, \varphi, \varphi_1, \varphi_2\rangle = g(\varphi_1, \xi, \varphi_2, \varphi, \theta, \varphi_3, \zeta, \varphi_4) |N, 0, 0\rangle, \quad (15)$$

which can be expressed as

$$\begin{aligned} |\xi, \theta, \varphi, \varphi_1, \varphi_2\rangle &= \sum_{j_1=0}^N e^{i\varphi(N-j_1)} \sin^{j_1}(\theta) \cos^{(N-j_1)}(\theta) \binom{N}{j_1}^{1/2} \\ &\times \sum_{j_2=0}^{j_1} e^{ij_2\varphi_2} e^{i\varphi_1(j_1-j_2)} \sin^{j_2}(\xi) \cos^{(j_1-j_2)}(\xi) \binom{j_1}{j_2}^{1/2} |N-j_1, j_1-j_2, j_2\rangle. \end{aligned} \quad (16)$$

This parameterization of the SU(3) coherent state includes an arbitrary phase.

QUANTUM DYNAMICS OF THE SYSTEM

Analytical solutions

Let the initial state $|\psi(0)\rangle$ be an arbitrary SU(3) coherent state. The state $|\psi(t)\rangle$ for arbitrary time t may thus be given as

$$\begin{aligned} |\psi(t)\rangle &= \sum_{j_1=0}^N e^{i\varphi(N-j_1)} \sin^{j_1}(\theta) \cos^{(N-j_1)}(\theta) \binom{N}{j_1}^{1/2} \sum_{j_2=0}^{j_1} e^{ij_2\varphi_2} e^{i\varphi_1(j_1-j_2)} \sin^{j_2}(\xi) \cos^{(j_1-j_2)}(\xi) \binom{j_1}{j_2}^{1/2} \\ &\times \exp[-2i\chi t (N^2/3 + j_1^2 + j_2^2 - j_1(N+j_2))] |N-j_1, j_1-j_2, j_2\rangle, \end{aligned} \quad (17)$$

under the Hamiltonian evolution (10). The time-dependent element of Eq. (17) exhibits the periodic evolution of the state and suggests that the state evolves into superposition states periodically, by analogy with the SU(2) coherent

state superposition case[6], but with additional complexity due to the greater number of parameters and the higher dimension of the group manifold.

From Eq. (17), we observe that the recurrence time, for which the state evolves cyclically back into the original state, is given by $\tau \equiv \pi/\chi$ for all values of the irrep parameter N . At half the recurrence time, $\tau/2 = \pi/2\chi$, the state evolves into the superposition

$$|\psi(\tau/2)\rangle = \frac{1}{2}e^{-i\pi N^2/3} [-|\xi, \theta, \varphi, \varphi_1, \varphi_2\rangle + |\xi, \theta, \varphi, \varphi_1 + \pi, \varphi_2\rangle + |\xi, \theta, \varphi, \varphi_1, \varphi_2 + \pi\rangle + |\xi, \theta, \varphi, \varphi_1 + \pi, \varphi_2 + \pi\rangle], \quad (18)$$

for even N , or

$$|\psi(\tau/2)\rangle = \frac{1}{2}e^{-i\pi N^2/3} [|\xi, \theta, \varphi, \varphi_1, \varphi_2\rangle + |\xi, \theta, \varphi + \pi, \varphi_1, \varphi_2\rangle + |\xi, \theta, \varphi, \varphi_1 + \pi, \varphi_2\rangle + |\xi, \theta, \varphi, \varphi_1, \varphi_2 + \pi\rangle], \quad (19)$$

for odd N . At one-quarter of the recurrence time $\tau/4$, the state evolves into a superposition state with the exact form depending on the total number N . There are four types of superposition states at $\tau/4$, classified by the quantity $N \bmod 4$. The four types are given as the following,

1. If $N = 4n$, for n an integer,

$$\begin{aligned} |\psi(\tau/4)\rangle &= \frac{1}{4}e^{-i\pi N^2/6} \\ &\times \left[|\xi, \theta, \varphi, \varphi_1, \varphi_2\rangle + |\xi, \theta, \varphi, \varphi_1 + \pi, \varphi_2\rangle + |\xi, \theta, \varphi, \varphi_1, \varphi_2 + \pi\rangle + |\xi, \theta, \varphi, \varphi_1 + \pi, \varphi_2 + \pi\rangle \right. \\ &+ i \left(-|\xi, \theta, \varphi, \varphi_1, \varphi_2 - \frac{\pi}{2}\rangle - |\xi, \theta, \varphi, \varphi_1, \varphi_2 + \frac{\pi}{2}\rangle + |\xi, \theta, \varphi, \varphi_1 + \frac{\pi}{2}, \varphi_2 - \frac{\pi}{2}\rangle - |\xi, \theta, \varphi, \varphi_1 + \frac{\pi}{2}, \varphi_2 + \frac{\pi}{2}\rangle \right. \\ &+ |\xi, \theta, \varphi, \varphi_1 + \frac{\pi}{2}, \varphi_2 + \pi\rangle - |\xi, \theta, \varphi, \varphi_1 + \frac{\pi}{2}, \varphi_2\rangle + |\xi, \theta, \varphi, \varphi_1 + \pi, \varphi_2 - \frac{\pi}{2}\rangle + |\xi, \theta, \varphi, \varphi_1 + \pi, \varphi_2 + \frac{\pi}{2}\rangle \\ &\left. \left. - |\xi, \theta, \varphi, \varphi_1 - \frac{\pi}{2}, \varphi_2 - \frac{\pi}{2}\rangle + |\xi, \theta, \varphi, \varphi_1 - \frac{\pi}{2}, \varphi_2 + \frac{\pi}{2}\rangle - |\xi, \theta, \varphi, \varphi_1 - \frac{\pi}{2}, \varphi_2\rangle + |\xi, \theta, \varphi, \varphi_1 - \frac{\pi}{2}, \varphi_2 + \pi\rangle \right) \right] \quad (20) \end{aligned}$$

2. If $N = 4n + 1$,

$$\begin{aligned} |\psi(\pi/4\chi)\rangle &= \frac{1}{4}e^{-i\pi N^2/6} \\ &\times \left[|\xi, \theta, \varphi, \varphi_1 + \frac{\pi}{2}, \varphi_2 + \frac{\pi}{2}\rangle + |\xi, \theta, \varphi, \varphi_1 - \frac{\pi}{2}, \varphi_2 + \frac{\pi}{2}\rangle + |\xi, \theta, \varphi, \varphi_1 + \frac{\pi}{2}, \varphi_2 - \frac{\pi}{2}\rangle + |\xi, \theta, \varphi, \varphi_1 - \frac{\pi}{2}, \varphi_2 - \frac{\pi}{2}\rangle \right. \\ &+ i \left(-|\xi, \theta, \varphi, \varphi_1 + \frac{\pi}{2}, \varphi_2\rangle - |\xi, \theta, \varphi, \varphi_1 + \frac{\pi}{2}, \varphi_2 + \pi\rangle + |\xi, \theta, \varphi, \varphi_1 + \pi, \varphi_2\rangle - |\xi, \theta, \varphi, \varphi_1 + \pi, \varphi_2 + \pi\rangle \right. \\ &+ |\xi, \theta, \varphi, \varphi_1 + \pi, \varphi_2 - \frac{\pi}{2}\rangle - |\xi, \theta, \varphi, \varphi_1 + \pi, \varphi_2 + \frac{\pi}{2}\rangle + |\xi, \theta, \varphi, \varphi_1 - \frac{\pi}{2}, \varphi_2\rangle + |\xi, \theta, \varphi, \varphi_1 - \frac{\pi}{2}, \varphi_2 + \pi\rangle \\ &\left. \left. - |\xi, \theta, \varphi, \varphi_1, \varphi_2\rangle + |\xi, \theta, \varphi, \varphi_1, \varphi_2 + \pi\rangle - |\xi, \theta, \varphi, \varphi_1, \varphi_2 + \frac{\pi}{2}\rangle + |\xi, \theta, \varphi, \varphi_1, \varphi_2 - \frac{\pi}{2}\rangle \right) \right]. \quad (21) \end{aligned}$$

3. If $N = 4n + 2$,

$$\begin{aligned} |\psi(\tau/4)\rangle &= \frac{1}{4}e^{-i\pi N^2/6} \\ &\times \left[|\xi, \theta, \varphi, \varphi_1, \varphi_2\rangle + |\xi, \theta, \varphi, \varphi_1 + \pi, \varphi_2\rangle + |\xi, \theta, \varphi, \varphi_1, \varphi_2 + \pi\rangle + |\xi, \theta, \varphi, \varphi_1 + \pi, \varphi_2 + \pi\rangle \right. \\ &+ i \left(-|\xi, \theta, \varphi, \varphi_1 + \pi, \varphi_2 + \frac{\pi}{2}\rangle - |\xi, \theta, \varphi, \varphi_1 + \pi, \varphi_2 - \frac{\pi}{2}\rangle + |\xi, \theta, \varphi, \varphi_1 - \frac{\pi}{2}, \varphi_2 + \frac{\pi}{2}\rangle - |\xi, \theta, \varphi, \varphi_1 - \frac{\pi}{2}, \varphi_2 - \frac{\pi}{2}\rangle \right. \\ &+ |\xi, \theta, \varphi, \varphi_1 - \frac{\pi}{2}, \varphi_2\rangle - |\xi, \theta, \varphi, \varphi_1 - \frac{\pi}{2}, \varphi_2 + \pi\rangle + |\xi, \theta, \varphi, \varphi_1, \varphi_2 + \frac{\pi}{2}\rangle + |\xi, \theta, \varphi, \varphi_1, \varphi_2 - \frac{\pi}{2}\rangle \\ &\left. \left. - |\xi, \theta, \varphi, \varphi_1 + \frac{\pi}{2}, \varphi_2 + \frac{\pi}{2}\rangle + |\xi, \theta, \varphi, \varphi_1 + \frac{\pi}{2}, \varphi_2 - \frac{\pi}{2}\rangle - |\xi, \theta, \varphi, \varphi_1 + \frac{\pi}{2}, \varphi_2 + \pi\rangle + |\xi, \theta, \varphi, \varphi_1 + \frac{\pi}{2}, \varphi_2\rangle \right) \right]. \quad (22) \end{aligned}$$

4. If $N = 4n + 3$,

$$\begin{aligned}
|\psi(\tau/4)\rangle &= \frac{1}{4} e^{-i\pi N^2/6} \\
&\times \left[|\xi, \theta, \varphi, \varphi_1 - \frac{\pi}{2}, \varphi_2 - \frac{\pi}{2}\rangle + |\xi, \theta, \varphi, \varphi_1 + \frac{\pi}{2}, \varphi_2 - \frac{\pi}{2}\rangle + |\xi, \theta, \varphi, \varphi_1 - \frac{\pi}{2}, \varphi_2 + \frac{\pi}{2}\rangle + |\xi, \theta, \varphi, \varphi_1 + \frac{\pi}{2}, \varphi_2 + \frac{\pi}{2}\rangle \right. \\
&+ i \left(-|\xi, \theta, \varphi, \varphi_1 - \frac{\pi}{2}, \varphi_2 + \pi\rangle - |\xi, \theta, \varphi, \varphi_1 - \frac{\pi}{2}, \varphi_2\rangle + |\xi, \theta, \varphi, \varphi_1, \varphi_2 + \pi\rangle - |\xi, \theta, \varphi, \varphi_1, \varphi_2\rangle \right. \\
&+ |\xi, \theta, \varphi, \varphi_1, \varphi_2 + \frac{\pi}{2}\rangle - |\xi, \theta, \varphi, \varphi_1 \varphi_2 - \frac{\pi}{2}\rangle + |\xi, \theta, \varphi, \varphi_1 + \frac{\pi}{2}, \varphi_2 + \pi\rangle + |\xi, \theta, \varphi, \varphi_1 + \frac{\pi}{2}, \varphi_2\rangle \\
&\left. - |\xi, \theta, \varphi, \varphi_1 + \pi, \varphi_2 + \pi\rangle + |\xi, \theta, \varphi, \varphi_1 + \pi, \varphi_2\rangle - |\xi, \theta, \varphi, \varphi_1 + \pi, \varphi_2 - \frac{\pi}{2}\rangle + |\xi, \theta, \varphi, \varphi_1 + \pi, \varphi_2 + \frac{\pi}{2}\rangle \right). \quad (23)
\end{aligned}$$

The Q -symbol

In the previous section we have obtained analytical expressions of $|\psi(t)\rangle$ for two particular time values, $\tau/2$ and $\tau/4$. More generally however we can obtain the state analytically for all values of t . The density matrix $\rho(t)$ for the system may be written in terms of the pure state $|\psi(t)\rangle$ as

$$\rho(t) = |\psi(t)\rangle\langle\psi(t)|. \quad (24)$$

The Q -symbol for this state is given by[5]

$$Q(t) = \langle\xi, \theta, \varphi, \varphi_1, \varphi_2|\rho(t)|\xi, \theta, \varphi, \varphi_1, \varphi_2\rangle. \quad (25)$$

The arbitrary phase disappears in the calculation of $Q(t)$. It is thus convenient to employ the two relative phases $\phi_1 = \varphi_1 - \varphi$ and $\phi_2 = \varphi_2 - \varphi_1$. The Q -symbol for the state may thus be expressed as

$$Q(\xi, \theta, \phi_1, \phi_2 : \xi(0), \theta(0), \phi_1(0), \phi_2(0); t) = \left| \sum_{j_1=0}^N \sum_{j_2=0}^{j_1} S_{j_1, j_2}^N(\xi, \theta, \phi_1, \phi_2; t) \right|^2, \quad (26)$$

where

$$\begin{aligned}
S_{j_1, j_2}^N &= e^{-ij_1(\phi_1 - \phi_1(0))} (\sin \theta \sin \theta(0))^{j_1} (\cos \theta \cos \theta(0))^{N-j_1} \binom{N}{j_1} \\
&\times e^{-ij_1(\phi_2 - \phi_2(0))} (\sin \xi \sin \xi(0))^{j_1} (\cos \xi \cos \xi(0))^{N-j_1} \binom{j_1}{j_2} e^{-2i\chi t(j_1^2 + j_2^2 - j(N+j_2))}. \quad (27)
\end{aligned}$$

The Q -symbol depends on four periodic parameters, and therefore a plot of the Q -symbol would need to be embedded in five-dimensional space to be viewed. However, in order to view the plot we need to reduce the number of dimensions required for plotting the function. A simple way to plot the Q -symbol is to fix one parameter, for example by setting $\theta = \pi/2$. This corresponds to a *slice* of the Q -symbol, and the choice of where to slice depends on the features to be emphasized in the plot. A slice is a standard means for representing multi-dimensional figures; animation can be used, for example, to present the figure by ‘traveling’ through a sequence of slices. We will present an example in the following subsection.

An Example

The nonlinear $SU(2)$ oscillator generates superposition states from an initial $SU(2)$ coherent state and can generate a superposition of two distinct $SU(2)$ coherent states at a half of its recurrence time [6]. This superposition of two distinct $SU(2)$ coherent states results in two major peaks arising in the plot of the Q -symbol for the superposition state. Interference fringes midway between the two peaks arise due to the coherence properties of the superposition. These interference fringes can be clearly seen as dimples in a plot of the logarithm of the Q -symbol[21].

The superposition states we have seen in Eqs. (20-23) arise from the nonlinearity of the $SU(3)$ system. In this subsection, we wish to observe a manifestation of such a superposition by plotting the Q -symbol for the state. As

discussed in the previous subsection, we can reduce the dimension of the parameter space to two by obtaining a slice of the Q -symbol for the state. We consider an $SU(3)$ coherent state which is also an $SU(2)_{23}$ coherent state. This restriction to $SU(2)_{23}$ coherent states ensures that only a subset of the Q -symbol is explored, with this subset being a slice which can be plotted on the Poincaré sphere corresponding to the $SU(2)_{23}/U(1)$ coset space. An initial $SU(2)_{23}$ coherent state can be written as

$$\begin{aligned} |\psi(0)\rangle &= |\xi(0), \pi/2, \phi_1(0), \phi_2(0)\rangle \\ &= e^{-i\phi_1(0)N} \sum_{j_2=0}^N e^{i\phi_2(0)j_2} \sin^{j_2}(\xi(0)) \cos^{(N-j_2)}(\xi(0)) \binom{N}{j_2}^{1/2} |0, N-j_2, j_2\rangle \end{aligned} \quad (28)$$

A state in the $SU(2)_{23}$ subsystem stays in this subsystem under time evolution, so the factor of ϕ_1 becomes an arbitrary phase and disappears in the calculation of the Q -symbol. We now employ the notation \tilde{Q} to refer to a slice of the Q -symbol. In this notation, the reduced Q -symbol, with the initial condition (28), is given by

$$\begin{aligned} \tilde{Q}(\theta, \xi, \phi_2; t) &= \langle \xi, \theta, \phi_1, \phi_2 | \rho(t) | \xi, \theta, \phi_1, \phi_2 \rangle \\ &= \sin^{2N}(\theta) \sum_{p=0}^N \sum_{q=0}^N e^{-i(p-q)(\phi_2 - \phi_2(0))} (\sin(\xi) \sin(\xi(0)))^{p+q} (\cos(\xi) \cos(\xi(0)))^{(2N-(p+q))} \\ &\quad \times \binom{N}{p} \binom{N}{q} \exp[-2i\chi t(p-q)(p-q-N)] . \end{aligned} \quad (29)$$

The θ -component of the Q -symbol is time-independent with a fixed weighting of $\sin^{2N}(\theta)$. The optimal slice for observing the Q -symbol in the reduced ξ - ϕ_2 space is thus obtained by setting $\theta = \pi/2$.

With the initial condition $\xi(0) = \pi/4$, $\phi_2(0) = 0$, \tilde{Q} is simplified to

$$\begin{aligned} \tilde{Q}(\xi, \phi_2 : t) &= 2^{-N} \sum_{p=0}^N \sum_{q=0}^N e^{-i(p-q)\phi_2} \binom{N}{p} \binom{N}{q} \sin^{p+q}(\xi) \cos^{(2N-(p+q))}(\xi) \\ &\quad \times \exp[-2i\chi t(p-q)(p+q-N)] , \end{aligned} \quad (30)$$

and is numerically represented in Fig. 1 and Fig. 2. The time-dependent term in Eq. (30) implies that the time-evolution of the state is distinguishable in terms of the total number N . The product $(p-q)(p+q-N)$ is even for any p and q if N is odd, whereas it is not true for any even total number N . The recurrence time of the time evolution with an odd total number N is a half of the recurrence time with an even total number. We solve this evolution numerically and plot \tilde{Q} as it evolves for two values of the total number, $N = 9, 10$. Fig. 1 shows the time-evolution of \tilde{Q} for the state for even number $N = 10$; in contrast, Fig. 2 depicts the time-evolution of the \tilde{Q} for the state for odd number $N = 9$.

CONCLUSIONS

We have investigated the formation of superpositions of $SU(3)$ coherent states via a nonlinear Hamiltonian evolution. This evolution could be realized in terms of four-wave mixing in nonlinear optics or in terms of a nonlinear interaction between three independent modes of a Bose-Einstein condensate with nonnegligible nonlinear interactions between the separate, but overlapping, modes. The linear quantum tunneling term is allowed to vary independently of the nonlinear (collision) terms, and linear quantum tunneling is used to prepare the $SU(3)$ coherent state for N bosons in the three modes. Then this $SU(3)$ coherent state undergoes a nonlinear evolution into a superposition of $SU(3)$ coherent states.

We have obtained explicit expressions for the superposition of coherent states at one-half and one-quarter the recurrence time for this periodic evolution. Whereas superpositions of pairs of coherent states are obtained for half the recurrence time for Heisenberg-Weyl, $SU(2)$ and $SU(1,1)$ systems, the higher dimension of $SU(3)$ dynamics leads to much more complex and interesting superpositions even at half the recurrence time. The nature of the superposition depends on the quantity $N \bmod 4$, with N being the total quantum number. The state at some time t can be represented by the use of a Q -symbol representation. However, the multidimensional domain of the Q -symbol makes the visualization of this function challenging. We have suggested that the method of plotting slices of the Q -symbol is desirable in this respect. An example was provided where the dynamics could be restricted to $SU(2)_{23}$, which makes the plots quite clear and readily interpreted: a superposition of two $SU(2)$ coherent states is evident in these plots.

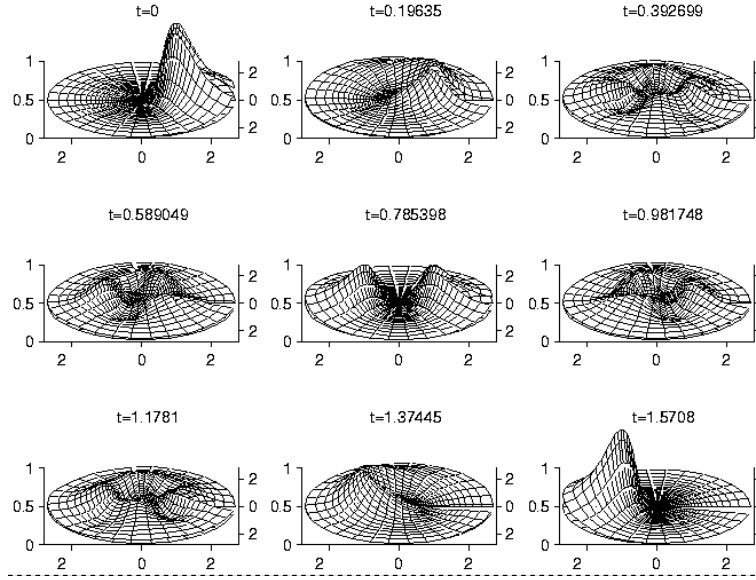


FIG. 1: $\tilde{Q}(\xi, \phi_2)$ is plotted at a certain time t with the use of the stereographical mapping. The origin corresponds the north pole of the spherical subdomain (ξ, ϕ_2) . Time flows from the left top figure at $t = 0$ to the right bottom figure at $t = \tau/2$. The recurrence time is twice as longer as the odd number case below.

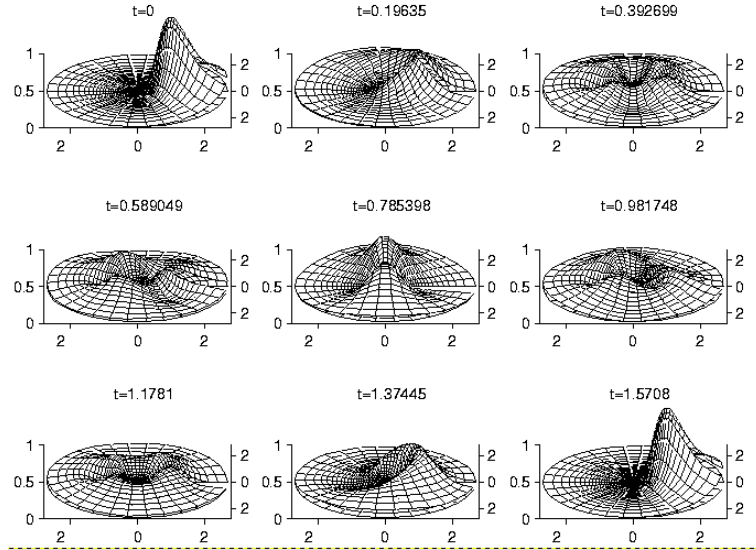


FIG. 2: $\tilde{Q}(\xi, \phi_2)$ is plotted at a certain time t with the use of the stereographical mapping. The origin corresponds the north pole of the spherical subdomain (ξ, ϕ_2) . Time flows from the left top figure at $t = 0$ to the right bottom figure at $t = \tau/2$. The recurrence time is a half of the even number case above.

This approach may be extended to $SU(n)$ coherent states by generalizing the Hamiltonian (1) to n interacting modes. However, the $SU(3)$ dynamics is the most relevant case to current physical realizations. Although nonlinear optics and Bose–Einstein condensation have been specifically mentioned, any three–boson system with the given nonlinear evolution (1) could yield superpositions of $SU(3)$ coherent states, provided that the initial state is itself an $SU(3)$ coherent state.

KN would like to thank G. J. Milburn for useful discussions. KN acknowledges the financial support of the Australian International Education Foundation (AIEF). This work has been supported by an Australian Research Council Large

Grant and by a Macquarie University Research Grant.

-
- [‡] Present address: School of Informatics, University of Wales, Bangor, United Kingdom
- [1] Yurke B and Stoler D 1986 Phys. Rev. Lett. **57**, 13
- [2] Bužek V and Knight P L 1995 Prog. in Optics **XXXIV** 1-158
- [3] Milburn G J 1986 Phys. Rev. A **33** 13
- [4] Sanders B C 1992 Phys. Rev. A **45** 6811; *errata* 1992 **46** 2966; Chai C L 1992 Phys. Rev. A **46** 7187; Wielinga B and Sanders B C 1993 J. Mod. Opt. **40** 1923; Ansari N A and Man'ko V I 1994 Phys. Rev. A **50** 1942
- [5] Perelomov A 1986 *Generalized Coherent States and Their Applications* (Springer Berlin)
- [6] Sanders B C 1989 Phys. Rev. A **40** 2417
- [7] Gerry C C 1987 Phys. Rev. A **35** 2146
- [8] Wang X-G, Sanders B C and Pan S-H 2000 J. Phys. A **33** 7451
- [9] Radcliffe J M 1971 J. Phys. A: Math. Gen. **4** 313
- [10] Arecchi F T, Courtens E, Gilmore R and Thomas H 1972 Phys. Rev. A **6** 2211
- [11] Yurke B, McCall S L and Klauder J R 1986 Phys. Rev. A **33** 4033
- [12] Nemoto K, Holmes C A, G J Milburn and Munro W J 2001 Phys. Rev. A **63** 013604.
- [13] Corney J F, Milburn G J and Zhang W 1999 Phys. Rev. A **59** 4630
- [14] Bollinger J J, Itano W M, Wineland D J and Heinzen D J 1996 Phys. Rev. A **54** R4649
- [15] Milburn G J, Corney J, Wright E M and Walls D F 1997 Phys. Rev. A **55** 4318
- [16] Sackett C A, Stoof H T C and Hulet R G 1998 Phys. Rev. Lett. **80** 2031
- [17] Cornish S L, Claussen N R, Roberts J L, Cornell E A and Wieman C E 2000 Phys. Rev. Lett. **85** 1795
- [18] Gnutzmann S and Kuš M 2000 J. Phys. A: Math. Gen. **31** 9871
- [19] Nemoto K 2000 J. Phys. A: Math. Gen. **33**, 3493
- [20] Rowe D J, Sanders B C and De Guise H 1999 J. Math. Phys. **40** 3604
- [21] Gagen M J 1995 Phys. Rev. A **51** 2715